PRE-PRINT

Gaze Estimation for Human-Robot Interaction: Analysis Using the NICO Platform

Matej Palider^a, Omar Eldardeer^b, Viktor Kocur^a

^aFaculty of Mathematics, Physics and Informatics, Comenius University, Bratislava ^bCONTACT UNIT, Italian Institute of Technology, Genoa

ARTICLE HISTORY

Compiled October 9, 2025

ABSTRACT

This paper evaluates the current gaze estimation methods within an HRI context of a shared workspace scenario. We introduce a new, annotated dataset collected with the NICO robotic platform. We evaluate four state-of-the-art gaze estimation models. The evaluation shows that the angular errors are close to those reported on general-purpose benchmarks. However, when expressed in terms of distance in the shared workspace the best median error is 16.48 cm quantifying the practical limitations of current methods. We conclude by discussing these limitations and offering recommendations on how to best integrate gaze estimation as a modality in HRI systems.

KEYWORDS

HRI, gaze estimation, deep learning, dataset

1. Introduction

Human gaze estimation is incorporated into many different Human-Robot Interaction applications [1,2]. This is mainly because of the importance of the gaze as a social non-verbal cue for interaction [3]. It drives many different social cognitive mechanisms (such as joint attention, intention prediction, and task coordination) and provides an explainable behaviour for others [4,5]. Affective states are also represented in the gaze behaviour [6]. The ability to perceive and understand the social cues affects the effectiveness and efficiency of the whole interaction experience. Gaze understanding and following is one of the earliest behavior mechanisms developed by infants to engage in different social communication scenarios [7].

Therefore, achieving high accuracy in gaze estimation is a key enabler to reach a seamless Human-Robot interaction task. Despite the significant progress of gaze estimation methodologies, these methods remain not fully evaluated in real human-robot interaction scenarios.

In this paper we present an applied evaluation for the latest gaze estimation methods in a standard HRI scenario, specifically when the human and the robot are engaged in a shared task space (e.g., table surface). With this paper, our contribution is an embodiment for gaze estimation methods using the NICO robotic platform [8], a dataset for

HRI gaze and an evaluation of the latest state-of-the-art off-the-shelf gaze estimation methods [9–12]. We make our dataset and evaluation code available.¹

Our analysis reveals that the accuracy of the evaluated gaze estimation methods in our scenario is similar to those reported on general-purpose gaze estimation datasets [13] with the best performing methods achieving errors slightly below 10°. However, when evaluated in terms of distance error on a shared work surface the best performing method [11] achieves median error of 16.48 cm, thus providing only a rough estimate of the point where the human directs their gaze towards. This limitation should be considered when gaze estimation is included as a modality in HRI tasks.

2. Related Work

2.1. 3D Gaze Estimation

3D gaze estimation attempts to estimate the 3D direction of human gaze from images. As input, cropped images of eyes [14–17], faces [9–11] or their combination [18] can be used. Some methods also focus on image sequences from videos to perform dynamic gaze estimation [12,19,20]. Most recent works are based on deep learning utilizing convolutional neural networks [10,11,14,15], transformers [12], or combined architectures [9]. Typically, the neural networks directly regress sparse representations of gaze direction. However, the full 3D eyeball geometry can also be modeled to improve accuracy [11].

2.2. Datasets

Training deep neural networks generally requires sufficient training data. Several gaze estimation datasets have been published in recent years. Some datasets [21,22] feature only limited distribution of gaze directions, include few human subjects, or are constrained to specific environments or applications. Gaze360 [13] aims to remedy these issues by collecting a dataset with a wide distribution of gaze directions featuring 238 human subjects in various environments. ETH-XGaze [23] focuses on broader variations in terms of pose and illumination. Datasets covering dynamical scenarios (gaze following) are also available [24,25].

To obtain the ground truth, setups with markers or projection systems and calibrated camera or camera rigs are commonly used. These HW requirements make the collection of large datasets very impractical. Some methods therefore aim to utilize datasets without annotated gaze. In [26] the authors curated a large collection of people looking at each other to provide a weak supervision signal to train gaze estimation networks. In a similar fashion 2D gaze information [12], or multi-view consistency [11] can be used to provide the training signal. Lack of real training data can also be supplemented by utilizing synthetically generated data [11,27,28].

 $^{^1}$ The dataset will be made available upon acceptance of the paper. The evaluation code is available at https://github.com/kocurvik/nico_gaze

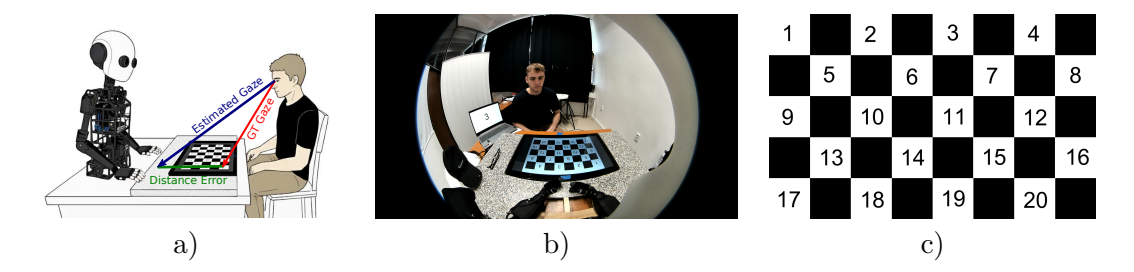


Figure 1. a) The experimental setup. Human participant sits in front of the robot. A display is embedded within the workspace shared by the robot and the participant. In our study we consider the distance between the estimated and ground truth gaze point on the shared work surface. b) View from the robot's left camera. c) The grid shown on the display.





Figure 2. Example of images used for stereo-calibration. Left: High field-of-view cameras are significantly distorted. Right: With known camera intrinsics it is possible to rectify the images.

3. Gaze Estimation from Robot's Perspective

The goal of this study is to evaluate the accuracy and usefulness of off-the-shelf gaze estimation methods in a standard HRI setup. We consider a setup where a human interacts with a humanoid robot in a shared working space with a dominant plane (e.g. a table). We implement a system which uses stereo-vision, face detection and gaze estimation methods to estimate the gaze point in the plane. In this section, we first provide details on our HW setup and then introduce various parts of our gaze estimation pipeline.

3.1. HW setup

In this paper we consider an HRI scenario with a humanoid robot. We use the NICO robotic platform [8] equipped with two See3CAM CU135 wide field-of-view cameras inside the robot's head. The robot's torso is placed on a table with a built-in display in the working area of the robot. The display is used to perform calibration of the robot camera poses. The humans interacting with the robot sit opposite of the robot and are directed to focus their gaze on individual squares on a grid displayed using the built-in display. The setup is shown in Fig. 1.

3.2. Camera Calibration

To infer the correct geometry using the robot's cameras, we perform camera calibration with a checkerboard pattern using [29]. We use images of the calibration pattern captured simultaneously by both cameras to also estimate their relative poses. The knowledge of the camera intrinsics allows us to rectify the images by removing the distortion caused by their lens (see Fig. 2). Since the relative poses of the cameras are also known, it is possible to triangulate points seen by both cameras to obtain a point

in 3D space.

In our setup the humans are looking at a display embedded within the work surface in front of the robot. A checkerboard grid with the white squares numbered is shown on the display (see Fig. 1). To evaluate the accuracy of the estimated gaze we need to know the transformation between two coordinate frames: C_c , which is the coordinate frame of the robot's left camera, and C_{π} , which is the coordinate frame associated with the plane of the display. In C_{π} , the coordinates of the checkerboard corners are $\vec{Y}_{i,j} = (si, sj, 0)$, where i and j denote the row and the column of the grid respectively and s denotes the metric square size (width and height). C_{π} is thus defined such that the work surface lies in the plane π defined by Z = 0.

To detect the plane position w.r.t. C_c , we first detect the chessboard corners in the image using [30] providing us with detected 2D checkerboard corners. We establish 2D-3D correspondences between the detected 2D corners and 3D points $\vec{Y}_{i,j}$. Using these 2D-3D correspondences and [31] we estimate the transformations between C_c and C_{π} defined by the rotation $R_{c\to\pi}$ and translation $\vec{t}_{c\to\pi}$.

3.3. Gaze Estimation

To estimate human gaze we test several off-the-shelf object detectors [9–12]. All of these methods use deep neural networks to detect human gaze direction. As outputs, these methods either provide a normalized 3D vector expressed in cartesian coordinates or the yaw and pitch of the gaze, which can be converted to a normalized 3D vector. More details regarding the implementation of the individual methods are provided in Section 5.1.

To estimate the gaze rays in C_c we first detect the bounding boxes of faces in images from both robots' cameras taken simultaneously. Using the known stereo-calibration, we can triangulate the center points of the detected bounding boxes. We denote this point as \vec{x} . Then we obtain the normalized gaze direction \vec{d} from a gaze-estimation network. The ray of the gaze in C_c is then $\{\vec{x} + \lambda \vec{d} \mid 0 \le \lambda\}$. Using the transformation between C_c and C_{π} we can transform the gaze ray into C_{π} denoting it as $\{\vec{x}' + \alpha \vec{d}' \mid 0 \le \alpha\}$, where $\vec{x}' = R_{c \to \pi} \vec{x} + \vec{t}_{c \to \pi}$ and $\vec{d}' = R_{c \to \pi} \vec{d}$. The point of intersection with the plane π in C_{π} is then found by solving for $\alpha = -x'_3/d'_3$, where x'_3 and d'_3 denote the third coordinate of vectors \vec{x}' and \vec{d}' respectively.

4. Evaluation Dataset

To evaluate the gaze estimation methods we have collected a dataset with human participants. We recruited six participants, five men and one woman in the age range 20-25. The participants were provided with information about the experiments and signed informed consent forms in accordance with a protocol approved by the Ethical Committee of the Faculty of Mathematics, Physics and Informatics, Comenius University Bratislava, with the number EKFMFI-23-02.

The participants were instructed to look at numbered white squares of the grid shown on the display in the workspace shared with the robot NICO. The individual white squares are marked with numbers from 1 to 20 (see Fig. 1). Each participant was instructed to look at a specific target square and while the administrator took images with the robot's cameras. The participants were asked to repeat this from different distances and positions two to three times for each square. For squares 11-20, the

participants were asked to wear glasses. In total our evaluation dataset contains 315 images from each camera.

4.1. Evaluation Metrics

To evaluate the gaze accuracy, we use the angle between the ground truth gaze direction and the gaze estimated by the network. The ground truth gaze is calculated using the estimated 3D position of the head and the 3D position of the center of the target square. We report the mean angular error of the predicted gaze directions.

We also calculate the error in terms of the estimated gaze point on the plane of the shared work surface (see Fig. 1a). Based on the estimated gaze and the estimated 3D head position, we calculate the point where the gaze ray intersects the work surface plane (see Sec. 3.3) and calculate the distance from the center of the target square. Since the distance can grow asymptotically with increasing angular gaze error we report the median distance instead of the mean, which may be biased by a few very large error measurements. We also report the proportion of the points estimated within 10, 20, and 50 cm distance error. We denote these metrics as Precision@Xcm.

5. Evaluation

5.1. Evaluated Gaze Estimation Methods

In our evaluation we include four recent methods: GazeTR [9], L2CS [10], 3DGazeNet [11], and Gaze3D [12]. We use their official implementations for evaluation. All methods first crop out faces using dedicated face detection networks. Gaze3D uses YOLOv5 trained on the CrowdHuman dataset [32], L2CS and 3DGazeNet use RetinaFace [33]. Since the official implementation for GazeTR does not provide a specific face detection, we use RetinaFace [33].

To determine the 3D position of the head we perform face detection on both the left and the right images from the robot's cameras. We triangulate the centers of the two boxes to obtain the 3D point. Since 3DGazeNet also estimates 2D coordinates of the eyes, we use the midpoints between the left and right eyes to calculate the 3D head position instead of relying on bounding box centers.

To evaluate GazeTR we use the GazeTR-Hybrid model trained ETH-XGaze dataset [23] and MPIIGaze [22]. The L2CS, 3DGazeNet and Gaze3D models were trained using the Gaze360 dataset [13]. Additionally, 3DGazeNet was trained using a semi-synthetic dataset ITWG-MV [11]. Gaze3D was also trained on the GFIE dataset [25].

L2CS, 3DGazeNet and Gaze3D return the gaze direction as the offset from the gaze directed directly at the camera center [13]. To estimate the gaze direction in the coordinate system of the camera, we correct the estimated yaw and pitch by adding the yaw and pitch from the 3D head position to the camera center to the estimates provided by the networks.

5.2. Results

The results of our evaluation are shown in Table 1. We also show the cumulative distribution functions of both the angular and distance errors in Figure 3. L2CS and 3DGazeNet perform the best in terms of the angular error. We note that both methods

Table 1. The results of the evaluated methods for the full dataset and its subsets with participants either wearing glasses or not wearing glasses.

Method	Mean Angular Error (°)	Median Distance (cm)	Distan @10cm	nce Precisio @20cm	on (%) @50cm
GazeTR [9]	14.69	22.85	17.14	43.17	86.03
L2CS [10]	9.65	17.66	28.89	58.41	89.52
3DGazeNet [11]	9.92	16.48	28.57	58.41	81.27
Gaze3D [12]	11.97	21.84	18.10	46.98	94.60

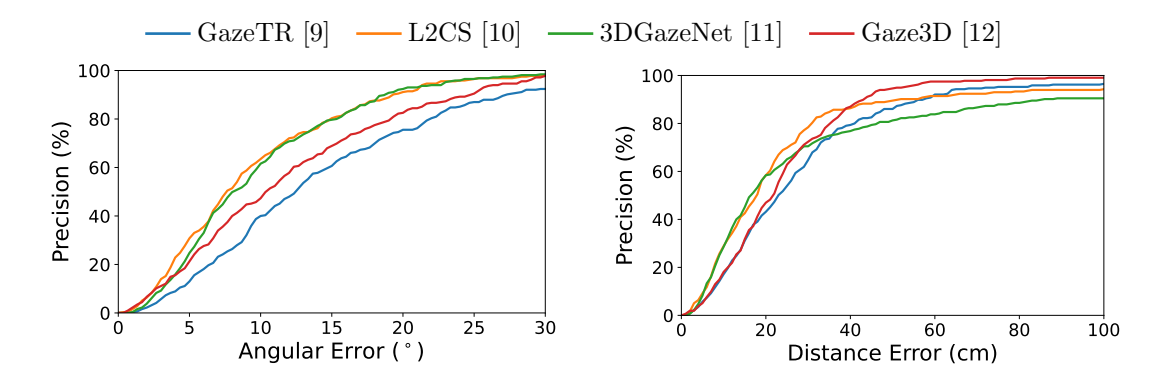


Figure 3. The cumulative distribution of the angular (left) and the distance (right) errors. The plots show the precision achieved (y-axis) given an error threshold (x-axis).

reach mean angular error similar to the error they achieve on the Gaze360 dataset [13] ($\sim 10^{\circ}$). In terms of the distance in the plane defined by the shared work surface, 3DGazeNet performs the best with a median distance of 16.48 cm. This suggests that localization of gaze within a shared work surface is limited in its accuracy.

In Figure 4, we plot the distributions of the estimated gaze directions in comparison to the ground truth. The distributions show that GazeTR underestimates the magnitutes of the yaw angle while Gaze3D overestimates the negative pitch.

5.3. Discussion

Based on the presented results, it is clear that current off-the-shelf gaze estimation methods can be beneficial in HRI systems, but their limitations must be considered. When used in a scenario similar to ours, the gaze information can only provide an estimate with a resolution of tens of centimeters. This can inform the potential layout of the shared space, such that this accuracy is sufficient to discriminate between objects or relevant portions of the shared working area. Conversely, gaze estimation networks could be used to provide only broader cues (e.g., whether the person is looking at the robot or at the shared workspace), which could still be useful. The inaccuracy could be accounted for and supplemented with information from other modalities in a multimodal perception system or by leveraging a broader context of the task. Performing multiple estimates using several images (video frames) could also lead to greater accuracy in aggregate or real-time information about the certainty of prediction accuracy.

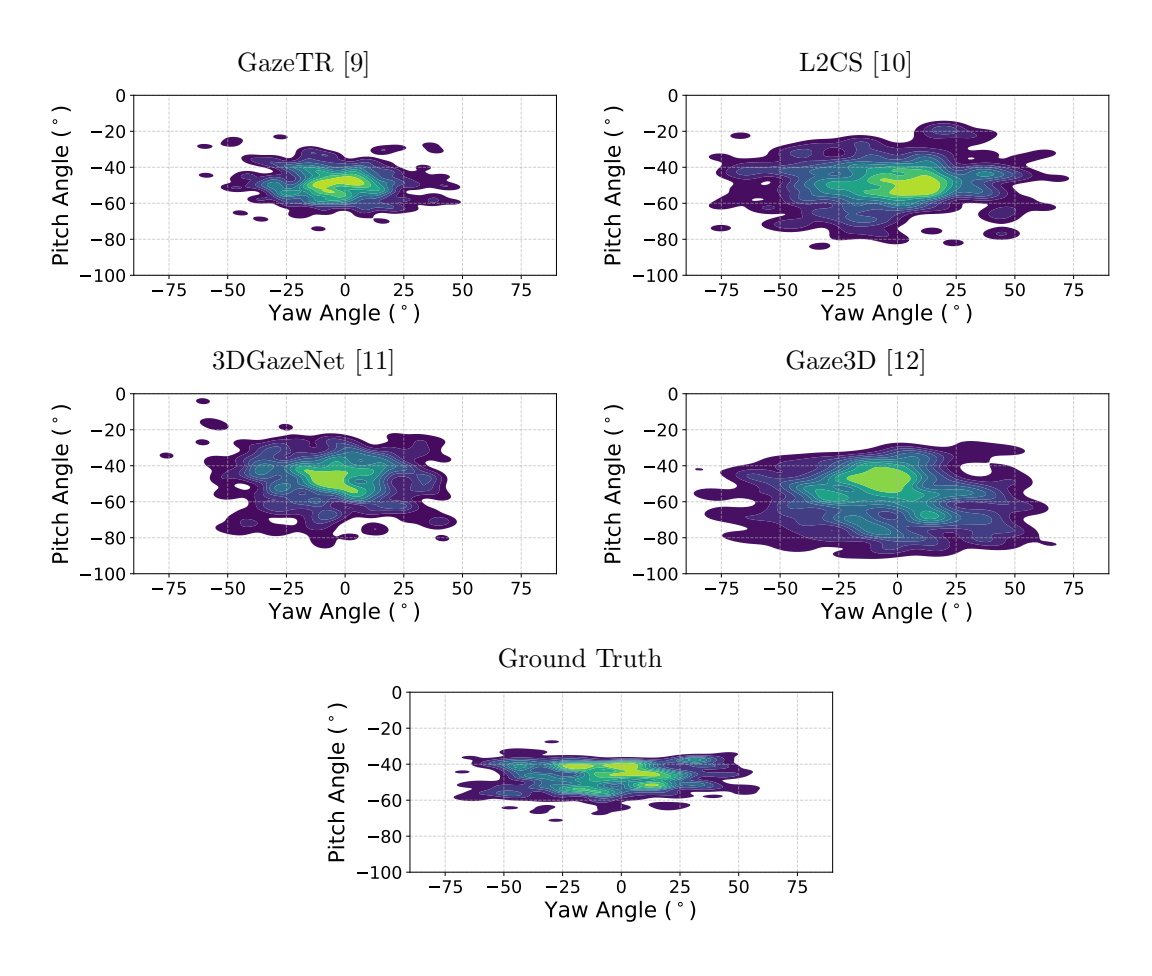


Figure 4. The distributions of the yaw and pitch angles for the ground truth and predicted gaze. For ground truth, we consider the direction from the head position estimated using RetinaFace [33] to the center of the target square. For visualization, we allow the pitch angles to go below -90°.

6. Conclusion

In this paper, we evaluate the accuracy of using off-the-shelf gaze estimation methods in an HRI scenario involving a working surface shared by a robot and a human. In order to perform the evaluation, we have collected an annotated dataset using the robotic platform NICO. We have evaluated four recent methods using our dataset. We found that the methods perform within the expected accuracy in terms of the mean angular error. However, when the estimated gaze is used to determine a specific gaze point in a planar working space shared by the robot and the human, the error within the plane expressed in terms of metric distance remains relatively high, with a 16 cm median error for the best performing method. Based on our findings, we provide several recommendations on how to incorporate off-the-shelf gaze estimation methods in HRI systems.

Our work has several limitations. As future work, our dataset could be extended to include a greater variety of participants, additional robotic platforms, or different scenarios. Additionally, the evaluation could be strengthened by also considering videos providing additional temporal context.

Data Availability Statement

The dataset will be made available upon acceptance. The evaluation code is available on https://github.com/kocurvik/nico_gaze.

Disclosure statement

The authors report there are no competing interests to declare.

Funding

The work presented in this paper was carried out in the framework of the TERAIS project, a Horizon-Widera-2021 program of the European Union under the Grant agreement number 101079338. This work was also supported by the Slovak Grant Agency for Science (VEGA), project no. 1/0373/23.

References

- [1] Admoni H, Scassellati B. Social eye gaze in human-robot interaction: a review. Journal of Human-Robot Interaction. 2017;6(1):25–63.
- [2] Palinko O, Rea F, Sandini G, et al. Eye gaze tracking for a humanoid robot. In: 2015 IEEE-RAS 15th International Conference on Humanoid Robots (Humanoids); 2015. p. 318–324.
- [3] George N, Conty L. Facing the gaze of others. Neurophysiologie Clinique/Clinical Neurophysiology. 2008;38(3):197–207.
- [4] Kleinke CL. Gaze and eye contact: a research review. Psychological bulletin. 1986; 100(1):78.
- [5] Mundy P, Block J, Delgado C, et al. Individual differences and the development of joint attention in infancy. Child development. 2007;78(3):938–954.
- [6] Merten J. Facial-affective behavior, mutual gaze, and emotional experience in dyadic interactions. Journal of Nonverbal Behavior. 1997;21(3):179–201.
- [7] Beier JS, Spelke ES. Infants' developing understanding of social gaze. Child development. 2012;83(2):486–496.
- [8] Kerzel M, Strahl E, Magg S, et al. Nico—neuro-inspired companion: A developmental humanoid robot platform for multimodal interaction. In: 2017 26th IEEE International Symposium on Robot and Human Interactive Communication (RO-MAN); IEEE; 2017. p. 113–120.
- [9] Cheng Y, Lu F. Gaze estimation using transformer. In: 2022 26th International Conference on Pattern Recognition (ICPR); IEEE; 2022. p. 3341–3347.
- [10] Abdelrahman AA, Hempel T, Khalifa A, et al. L2cs-net: Fine-grained gaze estimation in unconstrained environments. In: 2023 8th International Conference on Frontiers of Signal Processing (ICFSP); IEEE; 2023. p. 98–102.
- [11] Ververas E, Gkagkos P, Deng J, et al. 3dgazenet: Generalizing 3d gaze estimation with weak-supervision from synthetic views. In: European Conference on Computer Vision; Springer; 2024. p. 387–404.
- [12] Vuillecard P, Odobez JM. Enhancing 3d gaze estimation in the wild using weak supervision with gaze following labels. In: Proceedings of the IEEE/CVF Conference on Computer Vision and Pattern Recognition (CVPR); Jun.; 2025.
- [13] Kellnhofer P, Recasens A, Stent S, et al. Gaze360: Physically unconstrained gaze estima-

- tion in the wild. In: Proceedings of the IEEE/CVF international conference on computer vision; 2019. p. 6912–6921.
- [14] Park S, Spurr A, Hilliges O. Deep pictorial gaze estimation. In: Proceedings of the European conference on computer vision (ECCV); 2018. p. 721–738.
- [15] Cheng Y, Lu F, Zhang X. Appearance-based gaze estimation via evaluation-guided asymmetric regression. In: Proceedings of the European conference on computer vision (ECCV); 2018. p. 100–115.
- [16] Chen Z, Shi BE. Appearance-based gaze estimation using dilated-convolutions. In: Asian Conference on Computer Vision; Springer; 2018. p. 309–324.
- [17] Biswas P, et al. Appearance-based gaze estimation using attention and difference mechanism. In: Proceedings of the IEEE/CVF conference on computer vision and pattern recognition; 2021. p. 3143–3152.
- [18] Krafka K, Khosla A, Kellnhofer P, et al. Eye tracking for everyone. In: Proceedings of the IEEE conference on computer vision and pattern recognition; 2016. p. 2176–2184.
- [19] Park S, Aksan E, Zhang X, et al. Towards end-to-end video-based eye-tracking. In: European conference on computer vision; Springer; 2020. p. 747–763.
- [20] Palmero C, Selva J, Bagheri MA, et al. Recurrent cnn for 3d gaze estimation using appearance and shape cues. arXiv preprint arXiv:180503064. 2018;.
- [21] Funes Mora KA, Monay F, Odobez JM. Eyediap: A database for the development and evaluation of gaze estimation algorithms from rgb and rgb-d cameras. In: Proceedings of the symposium on eye tracking research and applications; 2014. p. 255–258.
- [22] Zhang X, Sugano Y, Fritz M, et al. Mpiigaze: Real-world dataset and deep appearance-based gaze estimation. IEEE transactions on pattern analysis and machine intelligence. 2017;41(1):162–175.
- [23] Zhang X, Park S, Beeler T, et al. Eth-xgaze: A large scale dataset for gaze estimation under extreme head pose and gaze variation. In: European conference on computer vision; Springer; 2020. p. 365–381.
- [24] Recasens A, Khosla A, Vondrick C, et al. Where are they looking? Advances in neural information processing systems. 2015;28.
- [25] Hu Z, Yang Y, Zhai X, et al. Gfie: A dataset and baseline for gaze-following from 2d to 3d in indoor environments. In: Proceedings of the IEEE/CVF Conference on Computer Vision and Pattern Recognition; 2023. p. 8907–8916.
- [26] Kothari R, De Mello S, Iqbal U, et al. Weakly-supervised physically unconstrained gaze estimation. In: Proceedings of the IEEE/CVF conference on computer vision and pattern recognition; 2021. p. 9980–9989.
- [27] Herashchenko D, Farkaš I. Appearance-based gaze estimation enhanced with synthetic images using deep neural networks. In: 2023 IEEE Symposium Series on Computational Intelligence (SSCI); IEEE; 2023. p. 129–134.
- [28] Doukas MC, Zafeiriou S, Sharmanska V. Headgan: One-shot neural head synthesis and editing. In: Proceedings of the IEEE/CVF International conference on Computer Vision; 2021. p. 14398–14407.
- [29] Zhang Z. A flexible new technique for camera calibration. IEEE Transactions on pattern analysis and machine intelligence. 2002;22(11):1330–1334.
- [30] Duda A, Frese U. Accurate detection and localization of checkerboard corners for calibration. In: British Machine Vision Conference; Vol. 126; 2018.
- [31] Collins T, Bartoli A. Infinitesimal plane-based pose estimation. International journal of computer vision. 2014;109(3):252–286.
- [32] Shao S, Zhao Z, Li B, et al. Crowdhuman: A benchmark for detecting human in a crowd. arXiv preprint arXiv:180500123. 2018;.
- [33] Deng J, Guo J, Ververas E, et al. Retinaface: Single-shot multi-level face localisation in the wild. In: Proceedings of the IEEE/CVF conference on computer vision and pattern recognition; 2020. p. 5203–5212.